Proceedings

Crack Initiation Mechanism and Crack Analysis of Walnut

Xiulan Bao[1,2], Biyu Chen [1,2], Peng Dai [1,2], Yishu Li [1,2] and Jincheng Mao [3,*

[1]   College of Engineering, Huazhong Agricultural University, Wuhan 430070, China;
      orchidbaoxl@mail.hzau.edu.cn
[2]   Key Laboratory of Agricultural Equipment in Mid-Lower Yangtze River, Wuhan 430070, China;
      35139904@qq.com
[3]   School of Mechanical and Electrical Engineering, Wuhan Institute of Technology, Wuhan 430073, China
[*]   Correspondence: jun—lan@163.com; Tel.: +86-138-7122-9154

Abstract: In order to achieve the complete separation of walnut shell and kernel, this paper aims to study the mechanical properties and cracking state of the shell surface of the Qingxiang walnut under unidirectional load. The goodness of fit (within 5%) of the spherical thin shell model was verified by the texture meter shell breaking experiment; A gradient decreasing distribution of shell stresses within the domain of load concentration forces was found by moment free theory and finite element simulation, and the internal forces are equal in all directions away from this domain; The fracture law of the shell surface along the grain was found by strength theory and solid fracture mechanics analysis; Finally, a walnut shell grasped by three-finger dexterous hand breaking experiment was designed to verify that the theoretical model in this paper is consistent with the actual walnut shell breaking state under unidirectional load, and the walnut cracks in the experiment are obvious, which is conducive to shell-kernel separation. The research results can provide a theoretical basis for the research and development of shell breaking machinery, and provide reference for the structural design and optimization of key components.

Keywords: walnut; broken shell; physical properties; crack; mechanical claws

1. Introduction

Walnut is a plant of the genus Juglans, which together with cashew, almond, hazelnut is known as the world's four dried fruit. Walnut kernels are rich in nutrients, such as protein, vitamins, cellulose, etc. Unsaturated fatty acids are high in content and protein content, which is very beneficial to the body and can strengthen the brain [1,2]. The weight of the shell in dried fruits such as walnuts is relatively large in proportion, and if they are processed directly, the edible part is small. Moreover, the hard shell is a serious obstacle to the extraction of effective components (pulp) in the processing. Walnut shell is mainly composed of lignin and hemicellulose, which is hard, difficult to peel with irregular appearance [3]. Moreover, the difference in size between different walnuts are large, the shell-kernel gap is small, and there is a complex diaphragm connection between the shell and kernel. These factors will lead to difficult separation of walnut shell and kernel completely, and it is also difficult to achieve a high complete kernel rate [4,5].

At present, the artificial shell breaking method with high cost and low efficiency is gradually replaced by high efficiency mechanical shell breaking equipment. In order to realize the mechanization of walnut shell breaking, domestic and international scholar have done a series of research [6–8]. Faroogh Sharifian, Kocturk, Ragab et al., found that appropriate moisture content and loading direction could greatly improve the processing efficiency and quality of walnut [9–11]. Wu found that two pairs of normal concentrated force can better achieve uniform shell rupture through a large number of tests [12]. Yan and Tu studied the mechanical properties of walnut shell breaking from the perspective

of finite element. These studies provide a theoretical basis for the development of walnut shell breaking machinery [13,14]. Ojolo et al., designed a rotary sheller, due to the large individual difference of walnut, the shelling effect was not ideal [15]. Li et al., developed a cone-basket walnut shell breaking device with good processing effect but low processing efficiency [16]. Liu et al., designed a flexible belt shearing extrusion shell breaking device which improve the shelling rate and reduce the broken kernel rate [17]. Ding et al., proposed a bionic knocking shell breaking method, developed a bionic knocking walnut shell breaking machine, which had high shell breaking efficiency but low complete kernel rate [18].

In order to improve the shell breaking efficiency and shell kernel separation rate, this paper explores the shell breaking state and mechanical properties of walnut shell under unidirectional load based on the physical characteristics of walnut shell. Walnut shell is a rotating shell in which two hemispherical shells are combined at the suture line (ridge line). Preliminary experiments found that when the walnut suture line (ridge line) was loaded, walnut shell and kernel will be divided into two parts directly from the suture. Therefore, this paper selects the shell surface except the ridge line to modelling and analyse, and studies the related characteristics of the continuous shell surface to provide a theoretical basis for the development of shell breaking machinery，and the three-finger dexterous hand grasping walnut impact shell breaking experiment is designed to verify. The research results can provide a theoretical basis for the research and development of shell breaking machinery, and provide reference for the structural design and optimization of key components.

2. Analysis and Verification of Walnut Characteristics Test

2.1. Materials and Instruments

The test subjects used Qingxiang thin-skinned walnuts. According to the horizontal diameter of the walnuts, three sizes of walnuts of large (35 ± 2 mm), medium (33 ± 2 mm), and small (27 ± 2 mm) were selected as the test walnut samples. The test instruments mainly include texture meter, digital vernier calliper (accuracy 0.02 mm) and digital thickness measuring instrument (accuracy 0.02 mm).
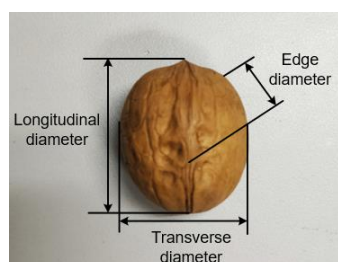
2.2. Experiments and Analysis

2.2.1. Sphericity Measurement

The measurement direction of triaxial size of walnut is shown in Figure 1 [19]. The three-axis dimensions of three specifications were measured by digital vernier calliper. Several measurements were measured in per specification. The measurement results were recorded and the sphericity was calculated by Formula (1).

$$S = \frac{\sqrt[3]{abc}}{d}(d = \max\{abc\}) \tag{1}$$

In the formula: S is the sphericity; a is the edge diameter (mm); b is the transverse diameter (mm); c is the longitudinal diameter (mm).

Figure 1. Schematic diagram of walnut diameter.

2.2.2. Sphericity Analysis

The average sphericity of large, medium, and small walnuts is 0.889, 0.883 and 0.904. Respectively, modelling the approximate spherical treatment of the walnut for the three specifications of walnut spherical degree are all above 88%.

2.2.3. Shell Thickness Measurement

Because the walnut shell is symmetrically distributed, seven points were selected to measure the shell thickness of half of the surface, as shown in the Figure 2. The thickness of each sampling point was measured by digital thickness measuring instrument. The three kinds of walnuts were divided into three groups and repeated the experiment of each group seven times. Get the average value of the results and make variance analysis of the results between the groups.
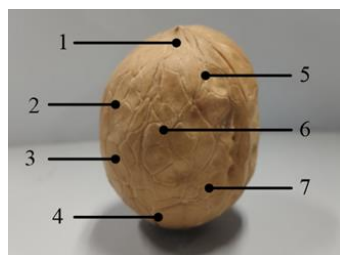

Figure 2. Schematic diagram of walnut shell taking point.

2.2.4. Shell Thickness Analysis

The measurement results of walnut shell thickness at different positions are shown in Figure 3. The figure shows that the shell thickness is related to the size and measurement point of the walnut. Therefore, two factors that may affect the shell thickness are selected: factor A (walnut size), factor B (different measurement points). Make the square-two-factor variance analysis of shell thickness; Analysis of variance results listed in Table 1, the results show that the P (test value) of the two factors are above 0.01, so considering the shell thickness of any position on the selected shell surface uniform in different sizes.
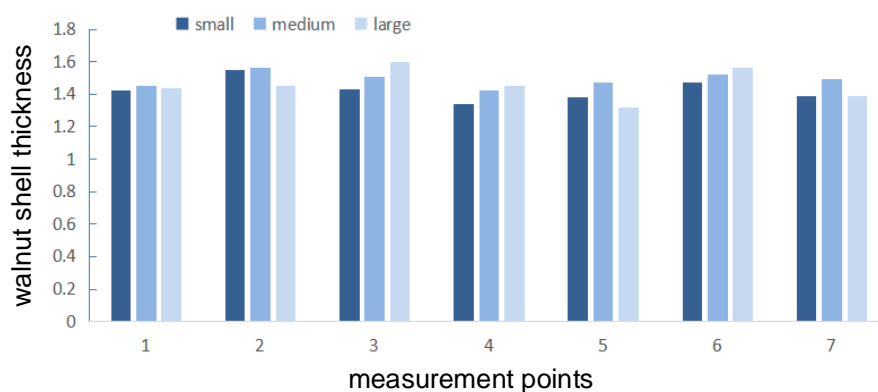

Figure 3. Walnut shell thickness at different positions.

Table 1. Two-factor variance analysis of shell thickness.

The Source of the Difference	The Sum of Squares	Degree of Freedom	Mean Square	*F*	*P*
Factor A	0.01384	2	0.00692	3.89	0.15
Factor B	0.05885	6	0.00981	2.99	0.04
Error	0.03710	12	0.00309		
Sum	0.10978	20			

From the conclusions in Sections 2.1 and 2.2, the walnut shell is approximately spherical and the shell thickness is uniform. Therefore, the walnut shell is simplified as a circular thin shell model in this paper, and the shell analysis is carried out by using the thin shell theory.

2.3. Verification of the Fit of the Thin Shell Model

The study shows that after the load is applied to the walnut, the stress is the largest at the load point, the deformation area is also concentrated near the load point, and the maximum deformation is at the load point, while the shell thickness at different positions varies, the corresponding compression stiffness is different, which means the mechanical properties are different. When the load is increased to a certain value under an external load, the walnut shell will be unstable, the walnut shell will be broken. According to elastic mechanics, the critical buckling pressure P_{cr} of spherical thin shells is calculated as follows:

$$P_{cr} = \frac{2E}{\sqrt{3(1-\mu^2)}} \left(\frac{h}{r}\right)^2 \tag{2}$$

where P_{cr}—critical pressure, GPa; E-Elastic Modulus, GPa; μ—Poisson's ratio; h—Shell thickness, mm; r—Radius, *mm*.

By experimentally measuring, walnut modulus of elasticity $E = 0.18$ GPa, Poisson's ratio $\mu = 0.38$, the shell thickness and the measured value of the radius ($r = min \{a, b, c\}/2$) and the elastic modulus, Poisson's ratio can be substituted into the above formula to calculate the critical stress for breaking the shell, then the calculated value of the breaking force can be obtained by $F = P \times S$ (take the approximate value of the compressed area $S = 100$ mm²), and the theoretical calculation value is as Table 2.

Taking the average value of the shelled walnuts measured force measured by the experiments on the texture meter as an experimental, and compared with the calculated value of the deviation values in the Table 2.

Table 2. Shell breaking force comparison table.

Specification / Shell-Breaking Force	Small (27 ± 2 mm)	Medium (33 ± 2 mm)	Large (35 ± 2 mm)
Calculated Value/N	317.3	303.7	312.7
Experimental Value/N	329.6	316.1	329.2
Bias/%	3.7	3.9	5.0

The results of the force comparison table show that there is a certain deviation between the fitting model of spherical thin shell and the actual situation in this paper, indicating that the actual shape, shell thickness distribution and other factors have a certain influence on the force characteristics of walnuts. Because the deviation of the results is less than 5%, the approximation and the fitting degree are at high-level.

3. Crack Analysis

During the experiment, it was found that under unidirectional (Y-direction) load, the load increased with the increase of the loading displacement. After reaching the strength limit, the walnut was unstable and fractured. In this process, the fracture first occurred at the maximum stress (the load point). With the load displacement continued to increase, the walnut shell continued to bend downward in the load direction. At the same time, the crack expanded outward from the beginning, ended at the maximum crack length (Figure 4).

Figure 4. Walnut crack.

3.1. Crack Type

According to the characteristics of force and displacement, cracks can be abstracted into three basic types: type I, type II, and type III. In the load concentration area, the load is the normal stress σ, and the direction is perpendicular to the surface of the walnut shell. The walnut will eventually rupture when pressed downwards, which is manifested as a crack caused by relative slippage occurred at the two surfaces, which is a type II crack. Outside the concentrated action, the crack mainly extends outward by the partial force pointing to each sides of the walnut, which is characterized as tearing from the middle and belongs to type I crack.

3.2. Crack Initiation

According to material mechanics, the brittle material will fail when the maximum principal normal stress reaches the unidirectional strength of the material under tensile or compressive load, which is the maximum normal stress yield criterion. The maximum normal stress yield criterion can be specified by the function as follows:

$$\sigma_M = MAX(|\sigma_x|, |\sigma_y|, |\sigma_z|) \tag{3}$$

where σ_M is the ultimate strength, σ_x, σ_y and σ_z are the stresses in the three principal axis directions.

When $\sigma_M < \sigma_u$, the material will not break, and when $\sigma_M \geq \sigma_M$, the material will fracture failure. In this walnut shell model, $\sigma_x = 0$, $\sigma_y = P_{cr}$, $\sigma_z = 0$, so the limit pressure strength $\sigma_u = |\sigma_y| = P_{cr}$; and under load P, $\sigma_1 = 0$, $\sigma_2 = -p$ (negative sign indicates pressure stress), $\sigma_3 = 0$, so $\sigma_M = |\sigma_2| = p$, when $p \geq P_{cr}$, that is, $\sigma_M \geq \sigma_u$, according to the maximum normal stress fracture criterion, the failure fracture of walnut shell occurs, and the initial crack is generated, that is, the crack initiation process.

3.3. Crack Expansion

There are generally two parameters in linear elastic fracture mechanics to measure the crack generation ability: energy release rate G and stress intensity factor K. When the energy release rate G or the stress intensity factor K exceeds its critical value: $G \geq G_C$ or $K \geq K_C$, it is considered that fracture occurs, which is the fracture criterion. According to fracture mechanics, stress intensity factor K is a measure of crack severity, which is related to crack size, stress, and geometric shape. This paper assumes that the mechanical

behavior of walnut shell is linear elastic, and using the knowledge of linear elastic fracture mechanics to analyze the cracks.

Studies have shown that cracks generated on a certain material tend to expand along the direction of lower toughness. For wood, the strength along the grain direction is lower than the strength in other directions, so wood cracks generally appear along the grain fracture [20]. The walnut shells in this article have similar properties, the longitudinal direction (Z-axis direction) can be speculated as the "long-grain direction" of the walnut shell, and the transverse direction (X-axis direction) is the "horizontal direction".

For the hypothesis of walnut shell "fracture along the grain", this calculation taking strength K_C to confirm the hypothesis. It can be seen from the foregoing that the stress intensity factor K is related to the applied stress and the crack length. According to linear elastic fracture mechanics, K is usually conveniently expressed as [21]:

$$K = FS\sqrt{\pi a} \tag{4}$$

where the parameter F is a function of the ratio a/b, which is related to the geometry; S is load stress; a is crack length.

In the case of the ratio of $\alpha = a/b < 0.4$, the expression of F is:

$$F = 1.12S\sqrt{\pi a} \tag{5}$$

For other cases where the $\alpha = a/b$, the expression of F is:

$$F = \sqrt{\frac{2}{\pi\alpha}\tan\frac{\pi\alpha}{2}} \left[\frac{0.923 + 0.199(1 - \sin\frac{\pi\alpha}{2})^2}{\cos\frac{\pi\alpha}{2}} \right] \tag{6}$$

3.3.1. The Longitudinal Direction

After measurement, substituted the longitudinal ratio $\alpha = a/b = 0.51$ into Formula (6), the longitudinal $F_Z = 1.48$ can be calculated. According to the experimental data, the average crack length of longitudinal shell breaking of walnut shell $a = 34.3$ mm, and the shell breaking force $S_Z = 310N$ in this paper. Substituting the data into Formula (4), the fracture toughness along the grain direction of walnut shell $K_{ZC} = 1.51$ MPa·m$^{1/2}$ in this paper.

3.3.2. The Transverse Direction

After measurement, substituted the transverse ratio $\alpha = a/b = 0.50$ into the formula (6), longitudinal $F_X = 1.47$ can be calculated. According to the experimental data, the average crack length of walnut shell $a = 20.1$ mm, and the shell breaking force $S_X = 468N$ in this paper. By substituting the data into the Formula (4), the transverse fracture toughness of walnut shell $K_{ZC} = 1.72$ MPa·m$^{1/2}$ can be got in this paper.
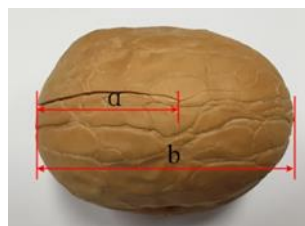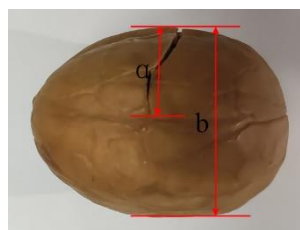

Figure 5. Width ratio of parallel crack. .

Figure 6. Width ratio of transverse crack.

The calculation results show that the transverse fracture toughness is greater than the longitudinal fracture toughness, so it can be confirmed that the longitudinal strength is smaller than the transverse strength, and the hypothesis that the longitudinal direction has the properties of "longitudinal fracture" can be proved.

According to experimental phenomena, most of the cracks are also longitudinal cracks. It can be inferred from the conclusion that no matter whether the initial cracks of walnuts are along the longitudinal direction, they are always affected by the fracture properties along the grain during the extension process, and the cracks will be longitudinally affected under this influence offset.

3.4. Crack Growth Rate

In the experimental phenomenon, the time for cracking of walnut shell under load compression is very short, so the process can't be observed by eyes. The value can be estimated according to the relevant formula. According to brittle solid fracture mechanics, under fixed boundary loading, the crack propagation rate is [22]:

$$v(c) = v_T f(c / c_0, \alpha) \tag{7}$$

where v_T is the limit speed; f is the function of scale one, which is calculated as:

$$f(c / c_0, 0) = 1 - c_0 / c \tag{8}$$

where c_0 is the initial crack length; c is the crack extension length;
The estimation of the limit speed is:

$$v_T \approx 0.38 v_1 \tag{9}$$

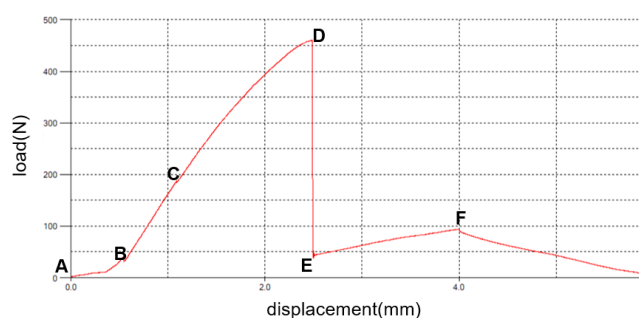where $v_1 = (E / \rho)^{1/2}$ is the longitudinal sound rate;

In this paper, the elastic modulus of walnut shell is 0.18 GPa, the density is 0.5 kg/m^3, the longitudinal sound wave rate $v_1 = 19$ km/s can be calculated, so the limit speed $v_T = 7.22$ km/s，the initial crack length c_0 is approximately 0, so $f \approx 1$, the crack expansion rate $v(c) \approx 7.22$ km·s^{-1}; In addition, the average length of cracks in this paper $a = 34.3$ mm, it can be estimated that the average time $t = a/v(c) = 4.75$ μs, and the crack completes the process from beginning to end in a very short time.

4. Shell Mechanics Analysis

4.1. Shell Deformation Process

The force-displacement of walnut shell during shell breaking on the texture meter is shown in Figure 7. From the shell breaking curve in Figure 7, the broken shell process of the walnut under Y-direction load can be summarized as follows: the AB section curve has a small slope and small fluctuations, mainly because the texture meter indenter enters the close contact stage with irregular surface of the walnut; the BC section is a straight line with a fixed slope *k*. According to the knowledge of engineering mechanics: *σ* = *Eε*. The elastic deformation stage is characterized by a linear relationship between the load and the strain. Therefore, the walnut produces elastic deformation under the load of this section, so the BC section is the elastic compression stage; The growth rate of slope of the

CD section decreases with the increase of the displacement of the transverse coordinate compared with BC section. According to the knowledge of material mechanics, the CD section not only produces elastic deformation, but also has partial plastic deformation, so the CD section is a mixed deformation stage of elastic deformation and plastic deformation. When the load value increases to σ_D, the load stress reaches the strength limit of walnut shell and thus fracture failure occurs, acting as brittle fracture. The EF section shows that the probe continues to compress walnut downward. Due to the instability fracture of walnut, the toughness has been reduced to a low value, so the load increased by unit displacement is small, and the slope k is small. After F point, the mass spectrometer load plate moves back to the initial position, and the load gradually decreases to zero.
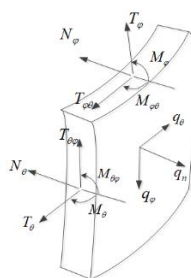

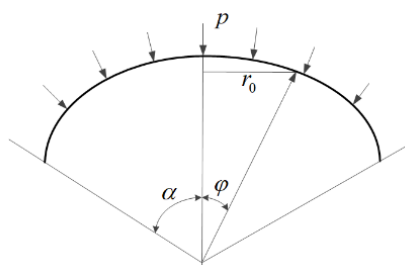**Figure 7.** Y Under load walnut breaking shell force—displacement curve.

4.2. Internal Force Analysis

Because of its small thickness, the bending capacity of thin shell is poor, and small bending moment will cause great stress and deformation, which has an important influence on the discussion of relevant parameters in the established mechanical model and formula. Therefore, the bending moment should be fully considered in the analysis of thin shell model. To solve this problem, the walnut shell is divided into concentrated force region and outer concentrated force region in this paper. The concentrated force region is around the region near the unidirectional load. Due to the existence of normal external load, there is a large bending moment in this region, which cannot be ignored. The region far from the concentrated force is the region remaining except the concentrated force region, and the bending moment generated in this region is small and negligible.

4.2.1. Outer the Concentrated Force Area

Figure 8. Diagram of the force of any section.

Figure 9. Force diagram.

Because the bending moment outer concentrated force region is negligible, the thin film theory (i.e., the momentless theory) is used for analysis. In a momentless state, only the stresses T_θ, T_φ and $T_{\theta\varphi}$ are considered, while torque M_θ, M_φ and $M_{\theta\varphi}$ are ignored. In equilibrium:

$$M_\theta = M_\varphi = M_{\theta\varphi} = N_\theta = N_\varphi = 0 \tag{10}$$

Under static balance conditions.

$$T_\varphi r_0 \sin\varphi = -\int_0^\varphi r_0 R(q_\varphi \sin\varphi - q_n \cos\varphi)d\varphi \tag{11}$$

The walnut shell is in any section, and $q_\varphi = 0$, $q_n = -p$, $R = r$, $r_0 = r\sin\varphi$.
Therefore available:

$$T_\varphi r \sin^2\varphi = -\int_0^\varphi r^2 \sin\varphi p \cos\varphi d\varphi \tag{12}$$

Thus available:

$$T_\varphi = -\frac{pr}{2} \tag{13}$$

Then by the formula:

$$\frac{T_\varphi}{R_1} + \frac{T_\varphi}{R_2} - q_n = 0 \tag{14}$$

Where R_1, R_2 is the radius of the primary curvature, $R_1 = R_2 = r$, thus available:

$$T_\theta = -\frac{pr}{2} \tag{15}$$
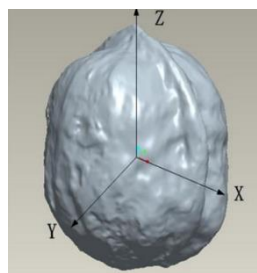
The result at T_θ, T_φ is equal in value, so the value of the internal force on any cross section of the walnut shell surface outer concentrated force area is equal, which can indicate that the walnut shell in this area has an isotropic property.

4.2.2. Concentrated Force Area

Due to the external load in concentrated force action area, there is a large bending moment can't be ignored. It can't be simply analyzed by the momentless theory, and the corresponding moment theory can be used for mechanical analysis. In this paper, the finite element analysis method is used to simulate the concentrated force area of walnut to obtain more intuitive and specific shell stress distribution.
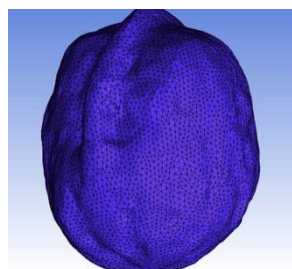
Modeling: using 3D scanner scanning to build a walnut 3D model as shown in Figure 10, and then the scanned 3D model into the finite element software;

Set material properties: Set the elastic modulus of the walnut model to 0.18 GPa, Poisson ratio is 0.3, density is 0.5 kg/m³.
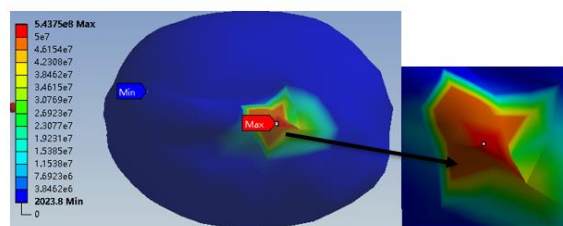
Figure 10. Walnut 3D Scan Model.

Meshing: Set the grid properties, the grid is given material properties, and then mesh the model as shown in Figure 11, mesh quality is greater than 0.3, mesh reasonable.
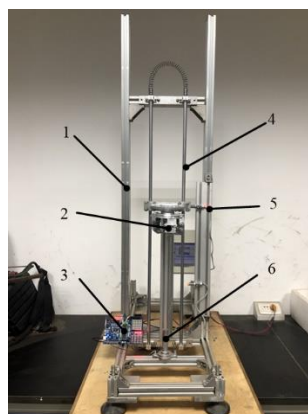

Figure 11. Meshing.

Force analysis: The contact load is added to the model, and the load is 100*N*, and then the simulation analysis is carried out. The stress cloud diagram obtained after the simulation analysis is shown in Figure 12. The stress cloud diagram intuitively reflects the stress distribution in the concentrated force area. Under the load, the shell stress is gradient distributed along the walnut shell, reaching the maximum at the concentrated point, and gradually decreasing away from the concentrated point.

Figure 12. Stress cloud map.

5. Three-Finger Manipulator Unidirectional Walnut Shell Breaking Experiments

According to the requirements of breaking walnut shell under unidirectional load, this paper designed a mechanical claw breaking test bench as shown in Figure 13, to carry out the actual walnut shell breaking test under unidirectional load.

Figure 13. Mechanical claw shell test bench. (**1**) frame; (**2**) three fingers mechanical claws; (**3**) microcontroller; (**4**) slider rail; (**5**) close switch; (**6**) impact table.

5.1. Experimental Procedure

On the test bench, the walnut sample was grabbed by a three-fingered mechanical claw, and then lifted the mechanical claw to the different heights of the calibration to make it fall freely along the slide rail until the walnut fell on the impact table to realize the application of unidirectional load.

According to momentum theorem:

$$F \cdot t = mv_2 - mv_1 \tag{16}$$

where F is the force; t is the action time; m is the mass; v_1 is the initial velocity; v_2 is the last velocity; both are vectors.

In this paper, the left part F is unknown, t is 0.01 s, the middle mass m on the right side of the formula is measured, the overall mass of the mechanical claws is 1.6 kg. In the experiment walnuts and impactors collide with almost no rebound, so take $v_2 = 0$, and v_1 can be measured by the following process: Two proximity switches are installed on the test bench framework, whose spacing is the calibration value X_0. The first proximity switch position is set as the starting position, and the second is set as the end position. The mechanical claw is placed at the starting position, and the microcontroller is started. Then the mechanical claw is released to make it fall freely along the sliding track. At this time, the timer program of the microcontroller is triggered to start timing. When the mechanical claw reaches the end position, the proximity switch is triggered again. At this time, the MCU stops the timing immediately after receiving the signal close to the switch, and the timing value t_0 is output and displayed. Then, the time for the mechanical claw to move from the initial position to the final position is t_0. Then, from the displacement formula $x = 1/2at^2$, the acceleration of the mechanical claw to fall freely on the sliding track is $a = 9.8$ m/s². Finally, the vertex of the impact table in the test bench is taken as the zero point, and the height value is calibrated with 10 cm as the unit length along the sliding track. At different height values h, the mechanical claws are released to fall freely along the sliding track until the walnuts collide with the impact table and break the shell. Then the velocity v during the impact can be calculated by the formula: $v^2 = 2ax$. Substituting a and h into the calculation, the obtained v value is the initial velocity v_1 in formula (16).

5.2. Test Results

Shell load force calculation: Based on the results of several experiments, the critical height of walnut shell breaking $h = 20$ cm. When the height is above 20 cm, the walnut will be seriously broken. When the height is below 20 cm, the walnut cannot break. Therefore, according to $v^2 = 2ax$, the initial velocity $v_1 = 1.98$ m/s can be obtained. According to formula (16), $t = 0.01$ s, $m = 1.6$ kg, $v_1 = 1.98$ m/s can be substituted into the formula to calculate the

Chem. Proc. **2022**, *4*, x FOR PEER REVIEW

12 of 13

load force $F = 316.8N$ in the process of collision. Comparisons show that the values agree with those obtained in the first chapter.

Walnut Crack: The walnut crack after the test is shown in the Figure 14. The crack propagation direction is consistent with the hypothesis of parallel fracture. The shell breaking effect is ideal and the complete kernel can be obtained.

Figure 14. Walnut crack and the complete kernel.

6. Discussions and Conclusions

In this paper, the spherical thin shell model was established based on walnut shell breaking experiment, and the model fitting degree was tested by the mechanical calculation of thin shell theory. The error was found to be within 5%, and consider the model is good. Based on this model, this paper draws the following conclusions through theoretical analysis and experiments:

(1) The walnut shell is divided into concentrated force domain and far from the concentrated force domain. In the outer concentrated force domain, the internal forces of the shell surface in all direction are equal by using the momentless theory. In the concentrated force domain, the finite element analysis method is used to intuitively show the gradient distribution of the internal force on shell from inside to outside.

(2) Walnut cracks include type Ⅰ and type Ⅱ cracks. According to the maximum stress yield criterion, it is determined that the crack initiation occurs at the place where the load is applied, and the crack propagation direction is calculated according to the fracture criterion and the stress intensity factor. Finally, the crack growth rate is estimated.

(3) The actual walnut shell breaking test under unidirectional load is designed and carried out. The actual walnut shell breaking force under unidirectional load is measured by the test, and the value is close to the theoretical value, and the crack propagation is consistent with the hypothesis of parallel fracture in this paper, which shows the reliability of the theoretical model in this paper. The research results can provide a theoretical basis for the research and development of shell breaking machinery, and provide reference for the structural design and optimization of key components.

Institutional Review Board Statement: Not applicable.

Informed Consent Statement: Not applicable.

Data Availability Statement: Not applicable.

Conflicts of Interest: The authors declare no conflict of interest.

References

1. Song, Y.; Wang, X.H.; Zhang, R.; Liu, C.H.; Yu, S.Q.; Gao, S.; Zhang, R.L. Comparison of Quality Differences Among Varieties of Walnut from Xinjiang. *J. Chin. Cereals Oils Assoc.* **2019**, *34*, 91–97.
2. Lu, J.; Zhao, A.Q.; Cheng, C. Nutritional composition and physiological activity of walnut and its development and utilization. *Food Mach.* **2014**, *30*, 238–242.
3. Aleksandra, V.C.; Marie-Christine, R.; Jacqueline, V.; Sara, K.; Arijana, M.; Draženka, K.; Estelle, B. Valorisation of walnut shell and pea pod as novel sources for the production of xylooligosaccharides. *Carbohydr. Polym.* **2021**, *263*, 117932.
4. Zhang, Z.H; Pei, D. *Walnut Science*; China Agricultural Press: Beijing, China, 2018.
5. Fu, Y.J.; Yang, S.; Wang, F.J.; Yuan, T.Q. Structural characterization of lignin from walnut shell. *J. For. Eng.* **2018**, *3*, 88–94.
6. Du, F.; Tan, T. Recent Studies in Mechanical Properties of Selected Hard-Shelled Seeds: A Review. *JOM* **2021**, *73*, 1723–1735.
7. Yang, Z.Q.; Yan, S.K.; Cui, K.B.; Wang, Q.H.; Sun, L.N.; Abulizi. A survey of green walnut processing and complete sets of equipment between the United States and China. *Food Mach.* **2019**, *35*, 228–232.
8. Liu, M.Z.; Li, C.H.; Cao, C.M. Research progress of key technology and device for size-grading shell-breaking and shell-kernel separation of walnut. *Trans. Chin. Soc. Agric. Eng.* **2020**, *36*, 294–310.
9. Ragab, K.; Pan, Z.L.; Griffiths. G; Atungulu. Size and moisture distribution characteristics of walnut and their components. *Food Bioprocess. Technol*. **2013**, *6*, 771–782.
10. Froogh, S.; Mohammadali, H.D. Mechanical behavior of walnut under cracking conditions. *J. Appl. Sci.* **2008**, *8*, 886–890.
11. Kocturk, B.O.; Gurhan, R. Determination of mechanical properties of various walnut according to different moisture levels. *J. Agric. Sci.* **2007**, *13*, 69–74.
12. Wu, Z.Y. Mechanical analysis of walnut shelling. *J. Nanjing Agric. Univ.* **1995**, *18*, 116–123.
13. Tu, C.; Yang, W.; Yin, Q.J. Optimization of technical parameters of breaking macadamia nut shell and finite element analysis of compression characteristics. *Trans. Chin. Soc. Agric. Eng.* **2015**, *31*, 272–277.
14. Yan, R.; Gao, J.; Zheng, J.H. Analysis of mechanical properties of walnut shell breaking based on workbench. *Agric. Mech. Res.* **2014**, *36*, 38–41.
15. Ojolo, S.J.; Damisa, O.; Orisaleye, J.I. Design and development of cashew nut shelling machine. *J. Eng. Des. Technol.* **2010**, *8*, 146–157.
16. Li, Z.X.; Liu, K.; Yang, L.L. Design and experiment of cone basket walnut shell breaking device. *J. Agric. Mach.* **2012**, *43*, 146–152.
17. Liu, M.Z.; Li, C.H.; Zhang, Y.B. Shell Crushing Mechanism Analysis and Performance Test of Flexible-belt Shearing Extrusion for Walnut. *Trans. Chin. Soc. Agric. Mach.* **2016**, *47*, 266–273.
18. Ding, R.; Cao, C.M.; Zhan, C. Design and experiment of bionic-impact type pecan shell breaker. *Trans. Chin. Soc. Agric. Eng.* **2017**, *33*, 257–264.
19. Zhang, H.; Shen, L.Y.; Lan, H.P.; Li, Y.; Liu, Y.; Tang, Y.R.; Li, W. Mechanical properties and finite element analysis of walnut under different cracking parts. *Int. J. Agric. Biol. Eng*. **2018**, *11*, 81–88.
20. Xu, B.H.; Wang, Y.X.; Zhao, Y.H. Advances in the study of the toughness of wood-striped fractures. *Mech. Pract.* **2016**, *38*, 493–500.
21. Norman, E.D.; Jiang, S.Y.; Zhang, Y.Q. *Mechanical Behavior of Engineering Materials*; China Machine Press: Beijing, China, 2015.
22. Law, B.; Gong, J.H. *Fracture Mechanics of Brittle Solids*; Higher Education Press: Beijing, China, 2010.